Ensuring Productive Resolution by the Junction-Resolving Enzyme RuvC: Large Enhancement of the Second-Strand Cleavage Rate

Jonathan M. Fogg and David M. J. Lilley*

CRC Nucleic Acid Structure Research Group, Department of Biochemistry, The University of Dundee, Dundee DD1 4HN, U.K.

Received August 10, 2000; Revised Manuscript Received October 19, 2000

ABSTRACT: RuvC is the principal junction-resolving enzyme of *Escherichia coli*, cleaving four-way DNA junctions created in homologous recombination. It binds with structural specificity to DNA junctions as a dimer, whereupon each subunit cleaves a phosphodiester bond of diametrically disposed strands. To generate a productive resolution event, these cleavages must be symmetrically located with respect to the point of strand exchange, and in the context of a branch-migrating junction, this requires near-simultaneous cleavage by the two subunits. Using a supercoil-stabilized cruciform as a substrate, we have analyzed the kinetics of strand cleavage. Coordinated bilateral cleavage is not essential in RuvC action, because a heterodimer comprising active and inactive subunits is active in unilateral cleavage. However, in operational terms, fully active RuvC appears to introduce simultaneous cleavages of two strands, because the rate of second-strand cleavage is accelerated by a factor of almost 150 relative to the first. We suggest that relief of strain following the first cleavage could lead to acceleration of subsequent cleavage, and show that DNA junctions rendered more flexible by the presence of strand breaks or bulges are subject to faster cleavage by RuvC. Cleavage of one strand of a junction generated in situ by the action of RuvC can accelerate cleavage at an intrinsically poor site by a factor of 500. Very large rate enhancement of second-strand cleavage by RuvC is likely to be essential to ensure productive resolution of a junction that is being actively branch migrated by the RuvAB machinery.

The four-way DNA junction is the central intermediate in homologous recombination (*1*−*5*). Resolution is brought about by a class of structure-selective nucleases, the junction-resolving enzymes [reviewed by White et al. (*6*)]. These enzymes exhibit strong structural selectivity for DNA junctions; in general, complexes of these enzymes with junctions are not displaced by a 1000-fold excess of duplex DNA. Examples of these enzymes have been isolated to date from bacteriophage-infected *Escherichia coli* (*7*, *8*), eubacteria (*9*, *10*), yeast (*11*−*13*), mammals (*14*) and their viruses (*15*), and most recently in euryarchaea (*16*) and the crenarchaea (*17*).

All the junction-resolving enzymes bind to DNA junctions in dimeric form, consistent with the two cleavages that are required for resolution of the branched species. However, to ensure productive resolution, two symmetrically disposed phosphodiester bonds must be cleaved. This suggests that some mechanism that coordinates the two cleavages is required, ensuring that they are correctly opposed. This is especially important in the context of a junction capable of branch migration where a junction could potentially reposition itself between cleavages. This would result in unopposed cleavages and hence an unresolved junction containing single-strand breaks in the arms.

Three kinds of outcome of the cleavage of a DNA junction by a resolving enzyme can be envisaged. First, the two cleavages could be simultaneous, such that one cannot occur without the other. Second, they could occur sequentially, but within the lifetime of the junction−enzyme complex. Last, they could be completely uncoordinated, and potentially brought about by different enzyme dimers. We have previously developed an assay to distinguish between these possibilities, based upon the cleavage of an appropriate cruciform structure stabilized within a supercoiled plasmid. This acts as a self-limiting substrate, since cleavage can release the negative supercoiling required to support the existence of the cruciform. Using this procedure, we have shown previously that the phage junction-resolving enzymes T4 endonuclease VII and T7 endonuclease I and the yeast junction-resolving enzyme CCE1 resolve cruciform-containing substrates into linear products (*18*−*20*), demonstrating that both cleavages take place within the lifetime of the enzyme−junction complex. It was also observed that for these enzymes the two cleavages were sequential, with the enzyme preserving the structure of the cruciform between cleavages and therefore preventing reabsorption of the cruciform into the nicked plasmid.

In the study presented here, we have analyzed the principal junction-resolving enzyme RuvC of *E. coli*. The results indicate that cleavage at the second site is accelerated by 2 orders of magnitude, much greater than that observed for other junction-resolving enzymes. As a result, the two cleavages become virtually simultaneous, thus ensuring productive resolution of the junction.

RESULTS

Principle of the Cruciform Assay. We have previously used a supercoil-stabilized cruciform structure as a self-limiting

* To whom correspondence should be addressed. Telephone: (44)-1382-344243. Fax: (44)-1382-201063. E-mail: dmjlilley@bad.dundee.ac.uk.

10.1021/bi001886m CCC: $19.00
Published on Web 12/01/2000

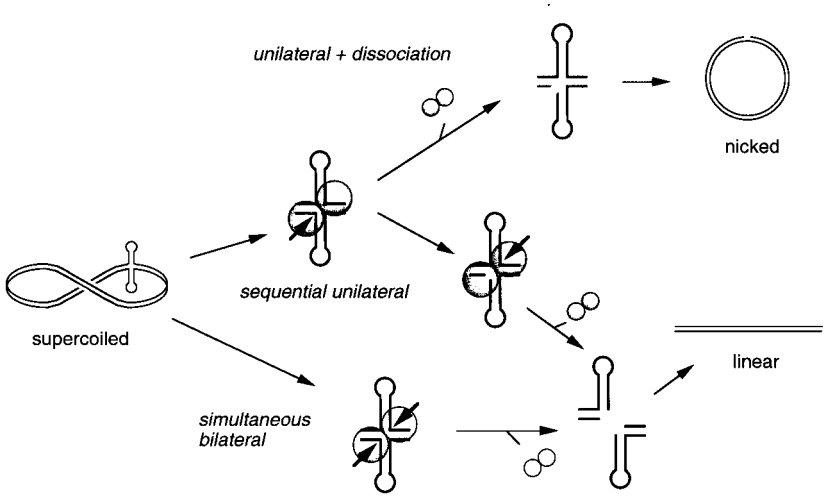

FIGURE 1: Possible products of resolution of a supercoil-stabilized cruciform structure. The cruciform structure formed by extrusion of an inverted repeat is stable only in a negatively supercoiled DNA molecule. If this is resolved by simultaneous bilateral cleavage (lower pathway), the result is a linear DNA species. Unilateral cleavage (upper pathway) would be expected to release the superhelical constraint, and thus destabilize the cruciform which would thereby be reabsorbed. If this occurs, no further cleavage is possible and the result is a nicked circular DNA species. However, if the nicked junction is tightly held by the enzyme such that the structure is preserved (center), a second cleavage might be possible, leading to a linear product. Thus, the linear product could be generated by either simultaneous bilateral cleavage or sequential unilateral cleavage with protein-mediated preservation of structure. If cleavage proceeds via the sequential mechanism, the nicked DNA intermediate might be detectable at early times.

substrate for junction-resolving enzymes. These structures are formed by intrastrand base pairing in inverted repeat sequences in DNA, and consist of a pair of hairpin loops extruded from the DNA (*21*−*23*). The region at the base of these loops is a four-way junction that can act as a substrate for Holliday junction-resolving enzymes (*24*, *25*). Since cruciform structures have significantly positive free energies of formation in linear DNA (*26*, *27*), they only enjoy a stable existence in negatively supercoiled DNA, where the free energy is supplied by the local unwinding of the DNA which leads to partial relaxation of supercoiling. Therefore, the cruciform only exists while the DNA remains supercoiled; any break in the DNA will release the supercoiling and thus destabilize the cruciform, leading to its reabsorption. This is important because it confers the character of a self-limiting substrate on the cruciform junction. If an enzyme introduces a unilateral cleavage such that the topological constraint is released, the cruciform will disappear and no further reaction will be possible. The product of the reaction under these circumstances would be nicked circular DNA. In contrast, linear DNA will be produced if bilateral cleavages are introduced into the DNA within the lifetime of the junction−enzyme complex. The two cleavages need not occur simultaneously, provided that the structure of the intermediate nicked junction is preserved by the bound protein. The two possible products and the supercoiled substrate are readily separated by agarose gel electrophoresis, allowing their easy identification. The different mechanisms of cleavage are illustrated schematically in Figure 1.

A Cruciform-Extruding Sequence with RuvC Cleavage Sites. To apply this analysis to RuvC, we required a plasmid containing a suitable cruciform that is stabilized by negative supercoiling. The choice of inverted repeat sequence is constrained by two requirements for RuvC cleavage. First, the enzyme cleaves most efficiently at the point of strand exchange in a four-way junction (*28*). To ensure that the cleavage site is located at the point of strand exchange, the extrusion of the cruciform must terminate at this point, and thus, the base located at the position 3′ of the cleavage must be different for the two sites. Second, RuvC exhibits a marked sequence preference for cleavage (*29*) with the optimal sequence being (A/T)TT↓(G>C=A) (*28*). We therefore used two efficiently cleaved sites (ATT↓G and ATT↓C); these would give cleavage rates as isolated junctions of 348×10^{-5} and 78.8×10^{-5} s^{-1} under single-turnover conditions at 37 °C (*28*). The sequence of the cruciform is shown in linear form in Figure 2A. The central part of the inverted repeat comprised an alternating adenine-thymine sequence which results in rapid extrusion kinetics and a lowered free energy of formation, thus facilitating formation of the cruciform (*30*).

The plasmid pRC1 containing the required inverted repeat was constructed by ligation of synthetic oligonucleotides between the *Bam*HI and *Eco*RI restriction sites of pAT153 (Figure 2B). Cleavage of supercoiled pRC1 with RuvC resulted in linearization of the DNA (Figure 2C, track 2); in contrast, the plasmid pCCE containing a different inverted repeat that lacked the RuvC cleavage sequences was not cleaved (data not shown). When pRC1 was first linearized by cleavage with *Ase*I followed by incubation with RuvC, no cleavage by the resolving enzyme was observed (Figure 2C, track 6) because the cruciform had been reabsorbed into linear DNA. The position of cleavage of supercoiled pRC1 by RuvC was analyzed by restriction analysis of the RuvC-linearized plasmid using *Sty*I, *Alw*NI, and *Ase*I for which single sites exist in pRC1 (Figure 2C, tracks 3−5). The lengths of the fragments that were generated were fully consistent with cleavage at the inverted repeat sequence.

Bilateral Cleavage of a Cruciform Junction by RuvC. Supercoiled pRC1 DNA was incubated with increasing concentrations of RuvC at 37 °C for 5 min, after which the reaction was terminated by the addition of EDTA to chelate magnesium ions (Figure 3). With increasing concentrations of RuvC, we observed the loss of supercoiled substrate together with a corresponding appearance of a linear plasmid. Very little nicked circular DNA is produced at any RuvC

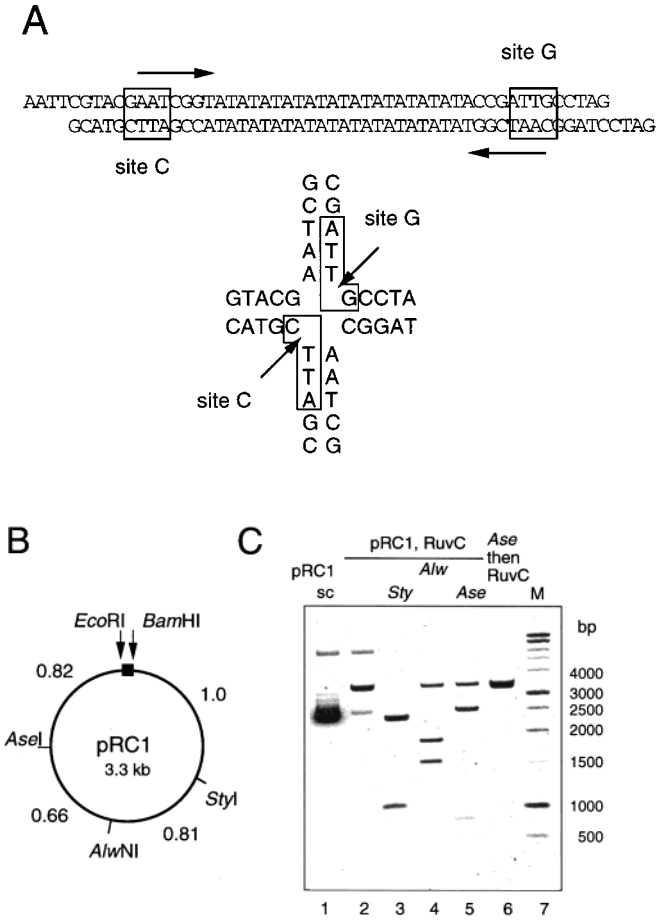

FIGURE 2: Plasmid pRC1 extrudes a cruciform that is resolved by RuvC. (A) The sequence of the inverted repeat. The sequence between the two arrows has 2-fold symmetry, and can form a perfect cruciform structure. The boxed sections are the ATTC and ATTG targets for RuvC cleavage. The middle section of the cruciform consists of alternating adenine-thymine sequence, which undergoes cruciform extrusion with a minimal kinetic barrier (*30*). The inverted repeat is drawn below as a cruciform. The RuvC target sequences are boxed, and the two cleavage sites are indicated by the arrows. The sites are named site C (ATTC) and site G (ATTG) as shown. (B) A circular map of pRC1, showing the restriction sites used in the characterization of the plasmid. The distances between sites are indicated (kilobase pairs). (C) Characterization of pRC1. Supercoiled pRC1 DNA is shown in track 1. Following incubation with RuvC, the DNA is substantially converted to the linear species (track 2). When this RuvC-generated linear DNA was subsequently cleaved to completion by unique site restriction enzymes *Sty*I, *Alw*NI, and *Ase*I (tracks 3−5, respectively), two linear subfragments were generated in each case. The sizes of these fragments were estimated using a semilogarithmic plot of mobilities against known sizes of marker DNA fragments (track 7; lengths given on right), giving values of 2.5 (2.3) and 1.0 (1.0) kbp for *Sty*I, 1.9 (1.8) and 1.6 (1.5) kbp for *Alw*NI, and 2.6 (2.5) and 0.8 (0.8) kbp for *Ase*I, respectively, where the values in parentheses have been calculated on the basis of the assumption of RuvC cleavage at the cruciform structure. Track 6 contains pRC1 that was linearized with *Ase*I and then incubated with RuvC.

concentration. This indicates that the cruciform undergoes bilateral cleavage during the lifetime of the enzyme−junction complex.

Near-Simultaneous Cleavages by RuvC Subunits. To generate the linear product, the two cleavages must occur within the lifetime of the junction−enzyme complex. Dissociation after the first cleavage would lead to loss of substrate, and this possibility is therefore excluded. However, the two cleavages might be simultaneous, or sequential with

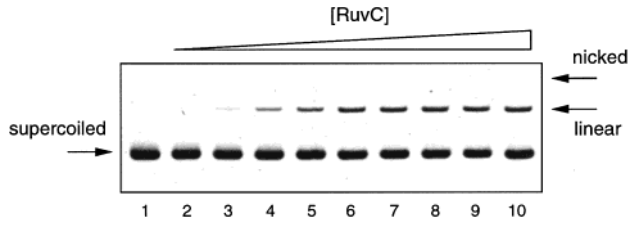

FIGURE 3: Cleavage of supercoiled pRC1 with increasing concentrations of RuvC. pRC1 was incubated with increasing concentrations of RuvC for 5 min. Under these conditions, the supercoiled DNA disappears and the linear product appears with an increasing level of digestion by RuvC, and nicked pRC1 is barely discernible. The concentrations of RuvC that were used were 0, 7.8, 15.6, 31, 63, 125, 250, and 500 nM and 1, 2, and 4 μM in tracks 1−10, respectively.

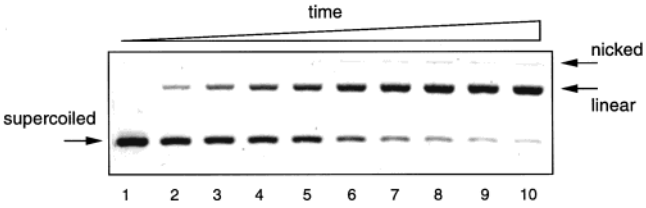

FIGURE 4: Cleavage of pRC1 with RuvC as a function of time. Supercoiled pRC1 (20 nM) was incubated with 1 μM RuvC at 47 °C. Aliquots were removed after increasing lengths of time, and the reaction was terminated. After deproteinization, the products were separated by electrophoresis in an agarose gel to resolve the nicked, linear, and supercoiled plasmid (indicated right). The gel was stained using ethidium bromide, and DNA species were visualized by fluorography. The times of reaction were 0, 15, 30, 45, 60, 120, 180, 240, 300, and 360 s in tracks 1−10, respectively.

an enzyme-stabilized nicked junction as an intermediate. We have shown previously that for CCE1 the cleavages are introduced sequentially, with the enzyme maintaining the structure of the cruciform junction between cleavages (*20*). This was demonstrated by the observation of a transient nicked species at very early times in the cleavage reaction. To test whether this was the case for RuvC, we studied the cleavage of pRC1 with a fixed concentration of RuvC as a function of time (Figure 4). Unlike other resolving enzymes that were tested, the only product observed was linear DNA even at the shortest time points. The very small amount of open-circular DNA (<5%) remained unchanged throughout the reaction. The absence of a unilaterally cleaved intermediate indicated that the two cleavages are apparently simultaneous.

Independent Cleavage Activity of RuvC Subunits. The failure to observe a transient nicked intermediate could result if the two subunits were functionally linked in some manner, such that one cleavage could not occur without cleavage at the opposite site. This would generate truly simultaneous cleavage. We therefore examined the ability of RuvC to generate unilateral cleavage in the absence of cleavage by its partner subunit, using a heterodimer formed from one active and one inactive protein. We incubated supercoiled pRC1 with a fixed concentration of wild-type RuvC to which was added increasing concentrations of an inactive mutant RuvC D7A (Figure 5); it is known that subunit exchange occurs in RuvC under these conditions (*31*) so that a fraction of active−inactive heterodimer enzyme will result. We observed the generation of an increasing fraction of nicked circular product as the proportion of inactive enzyme (and

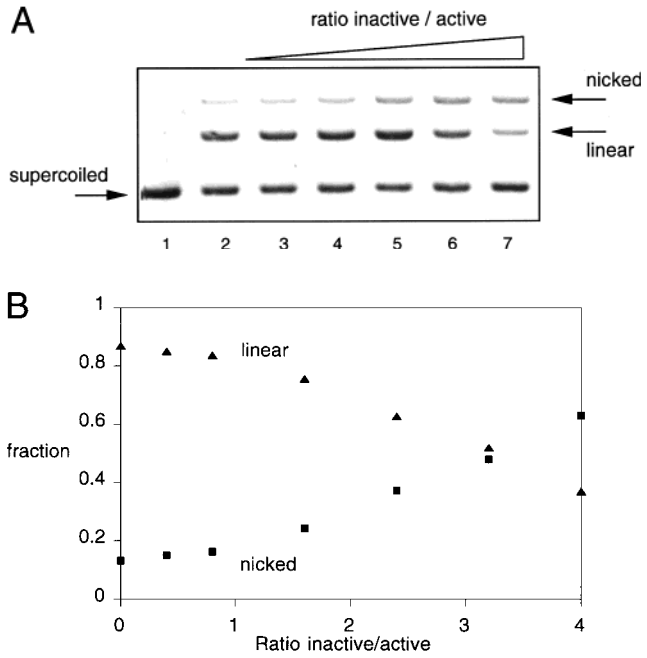

FIGURE 5: (A) Formation of nicked DNA by an active−inactive heterodimer of RuvC. A fixed concentration of wild-type RuvC (250 nM) was mixed with an increasing concentration of inactive RuvC D7A to generate the molar ratios given below. pRC1 was incubated with the mixtures of wild-type and inactive RuvC for 10 min at 47 °C. The molar ratios of inactive/active RuvC were 0, 0.4, 0.8, 1.6, 2.4, 3.2, and 4 in tracks 1−7, respectively. (B) Quantification of the linear and nicked DNA product as a function of the proportion of inactive RuvC. The main product is linear DNA (▲) at low molar ratios of inactive RuvC, but the proportion of nicked product rises as the mole fraction of inactive RuvC increases (■). This demonstrates that the active−inactive heterodimer of RuvC generates unilaterally cleaved DNA, indicating that an active RuvC monomer can function in combination with an inactive subunit.

hence the proportion of active−inactive heterodimer) rose. This was not due to a contaminating nuclease in the preparation of RuvC D7A, since incubation of pRC1 with RuvC D7A alone did not result in cleavage (data not shown). Thus, we conclude that simultaneous cleavage between subunits is not essential, and that one active site can function normally in the presence of a completely inactive partner subunit.

Interaction between Opposed Cleavages in a Junction. The near simultaneity of cleavages in a cruciform junction indicates that cleavage at the initial site leads to a marked acceleration of cleavage at the subsequent site; this is quantified in the Discussion below. We have therefore examined the ability of different sites within a DNA junction to influence the rate of cleavage at the diametrically opposed site (Figure 6). We have examined the rates of RuvC cleavage under single-turnover conditions for a series of junctions generated by the hybridization of four synthetic oligonucleotides. These were constructed to have b and r strands (i.e., those that become cleaved when the two sites are attacked by RuvC) of different lengths so that the products of cleavage at the two sites could be distinguished by electrophoresis in the same gel. The results are summarized in Table 1.

The b strand site in junction RCUNC1 has one of the critical central thymine bases replaced with guanine (i.e., the sequence is ATG↓G), and this would consequently be a very poor RuvC site in isolation (*28*). However, the opposing site on the r strand is the optimal RuvC cleavage site (ATT↓C). As a result, cleavage at the nominally poor b strand site is accelerated by a very large factor. This site becomes cleaved almost 500-fold faster when it is paired with the best RuvC sequence (ATT↓C in junction RCUNC1), compared to the situation where the optimal site is replaced with a poor site (GCC↓T in junction RCUNC2).

It was also observed that the rate of cleavage at the optimal sequence could be influenced by the opposing sequence to some degree. Thus, cleavage was 2 times faster when the opposing sequence was ATG↓G (junction RCUNC1, containing three out of four of the optimal bases) than when it was GCC↓T (junction RCUNC3, containing no matches). When the opposing site was changed to ATT↓C (junction RCUNC4), the rate was accelerated 15-fold.

However, not all sequences can be rescued by the presence of an opposing optimal RuvC sequence. The GCC↓T sequence of junction RCUNC3 is not cleaved efficiently despite the presence of the optimal sequence opposite, indicating that there are still sequence-specific interactions required for the second cleavage to proceed efficiently. The efficient cleavage of the r strand site in RCUNC3 is further evidence of the ability of the RuvC subunits for independent action. However, the very efficient cleavage of junction RCUNC4, which contains two optimal RuvC sequences, suggests that the two subunits work most efficiently together, with a mutual interaction between them.

Effect of Displacing the Cleavage Site from the Point of Strand Exchange. Translocation of an optimal RuvC site with respect to the point of strand exchange can lead to slower cleavage at a position displaced from the exchange point (*28*). We found that under such circumstances the optimal site could still accelerate an opposing RuvC cleavage, but to a lesser extent than when the site is optimally located, i.e., with cleavage at the point of strand exchange. Moreover, cleavage at the opposed position now occurred at three places, i.e., at the point of strand exchange (rate of 30.9×10^{-5} s^{-1}), and displaced one nucleotide (5.9×10^{-5} s^{-1}) or two nucleotides (41.1×10^{-5} s^{-1}) in the 3′ direction. Thus, the position of cleavage at the optimal site affects that of the opposed site.

Effect of a Strand Break on the Rate of Cleavage at an Opposite Site. It is clear that RuvC cleavage at one site in a junction can profoundly affect the rate of cleavage at the opposite site. This could result from the structural consequences of introducing a strand break into one side of the junction. We examined this possibility further by constructing four-way DNA junctions containing a pre-existing strand break at the point of strand exchange. A modified version of RCUNC1 was created containing a break in the b strand at the point of strand exchange. The rate of RuvC cleavage of the r strand was found to increase by 8-fold (rate of 6420×10^{-5} s^{-1}) compared to that of the corresponding intact junction (Figure 7).

Effect of Oligoadenine Bulges on the Rate of Cleavage at an Opposite Site. Acceleration of RuvC cleavage resulting from the presence of a strand break could be a result of increased flexibility of the junction within the enzyme−junction complex. To examine this possibility, we made modified versions of RCUNC1 and RCUNC3 containing an

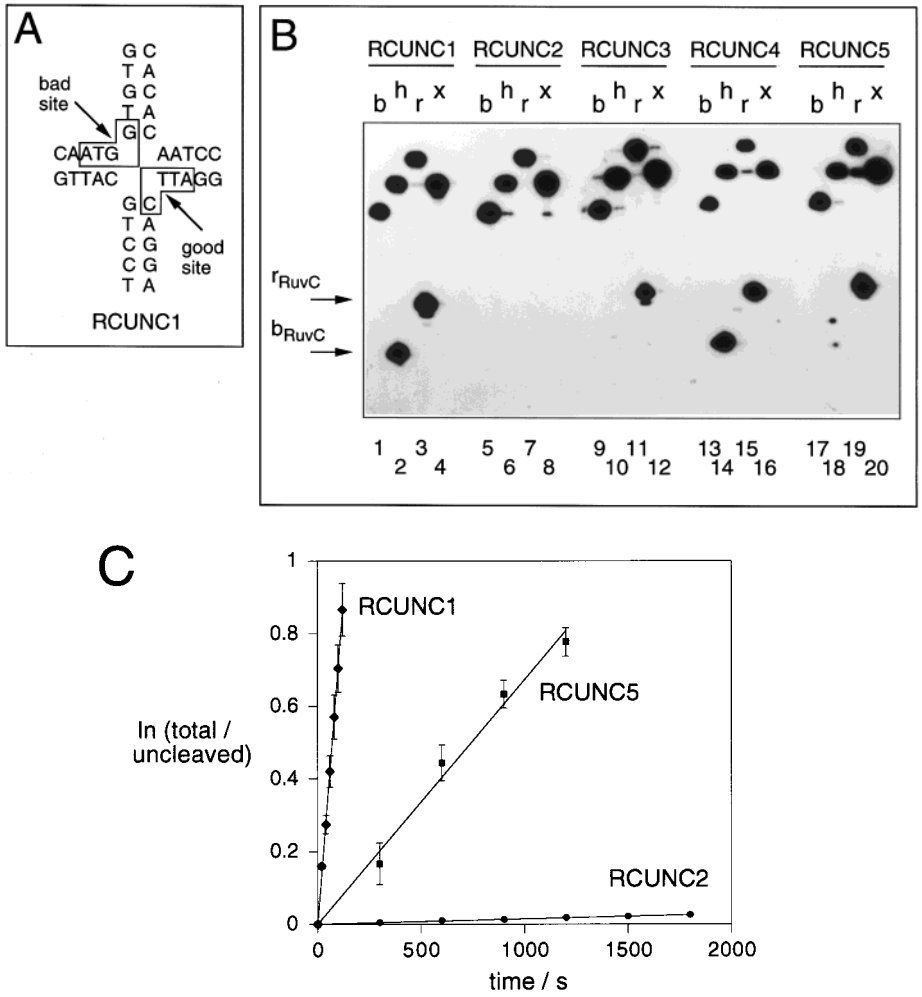

FIGURE 6: Influence between the cleavages at opposed sites within isolated DNA junctions. A series of DNA junctions was prepared by hybridization of four synthetic oligonucleotides (one of which was radioactively 5′-^{32}P labeled in each track) to present a variety of opposed sites of differing efficiency of cleavage by RuvC. (A) The central sequence of junction RCUNC1. This junction contains a site that is rapidly cleaved by RuvC (ATT↓C) opposing one (ATG↓G) that would be very poorly cleaved in isolation. (B) The junctions were incubated with RuvC under single-turnover conditions, and the products were analyzed by gel electrophoresis under denaturing conditions. The radioactive strands were visualized by autoradiography. Products of b strand cleavage (b_{RuvC}) and r strand cleavage (r_{RuvC}) by RuvC are indicated by the arrows on the left. These experiments reveal the large acceleration of RuvC cleavage at a given site when it opposes a good site for this enzyme. Thus, no RuvC cleavage is discernible at the b strand site in RCUNC2, whereas the same site becomes very well cleaved when it is opposed by a good RuvC site in RCUNC1. The results are summarized in Table 1. Tracks 1−4, 5−8, 9−12, 13−16, and 17−20 contain the results of RuvC cleavage on junctions RCUNC1, RCUNC2, RCUNC3, RCUNC4, and RCUNC5, respectively. Junctions were radioactively labeled on the b strand (tracks 1, 5, 9, 13, and 17), the h strand (tracks 2, 6, 10, 14, and 18), the r strand (tracks 3, 7, 11, 15, and 19), or the x strand (tracks 4, 8, 12, 16, and 20). (C) Plot of reaction progress as a function of time for RuvC cleavage of DNA junctions. The plot shows the rate of b strand cleavage in the ATGGTG site when it opposes an ATTCAG [RCUNC1 (◆)], GCCTAG [RCUNC2 (●)], or AATTCA site [RCUNC5 (■)]. The error bars are standard deviations of triplicate measurements.

oligoadenine base bulge in the b strand (interrupting the poorer RuvC site in each case). The results are summarized in Table 2. Not surprisingly, the presence of the bulge inhibited cleavage of the b strand for both sets of junctions. However, accelerated rates of cleavage were observed on the opposing strand. It was found that the presence of a single adenine at the point of strand exchange of the b strand of RCUNC1 accelerated the cleavage of the optimal site on the r strand by a factor of 5. Increasing the size of the oligoadenine bulge resulted in a smaller increase in cleavage rate relative to that of the unbulged version. It appears that only a small increase in flexibility is required to accelerate the cleavage at the second site, and larger bulges may cause steric hindrance within the complex.

Corresponding experiments with RCUNC3 showed that one- and two-base bulged junctions were cleaved more slowly than the unbulged junction. However three-, four-, and five-base bulged junctions were cleaved faster than the unbulged junction. This indicates that when there is no optimal sequence present, greater flexibility is required to accelerate cleavage at the opposing site.

Effect of Strand Breaks and Base Bulges on the Binding Affinity of RuvC. Electrophoretic retardation analysis was used to investigate the effect of the changes in junction structure on binding affinity of RuvC. In the presence of EDTA, the junction containing a strand break was bound very weakly, with an apparent K_D of 227 nM compared to the value of 2 nM for the fully intact junction. However, in the presence of 200 μM $MgCl_2$, the binding affinity was increased to 8 nM (K_D). This is consistent with the observation that nicked junctions are disordered in the absence of divalent metal ions but form a stacked X-structure in the

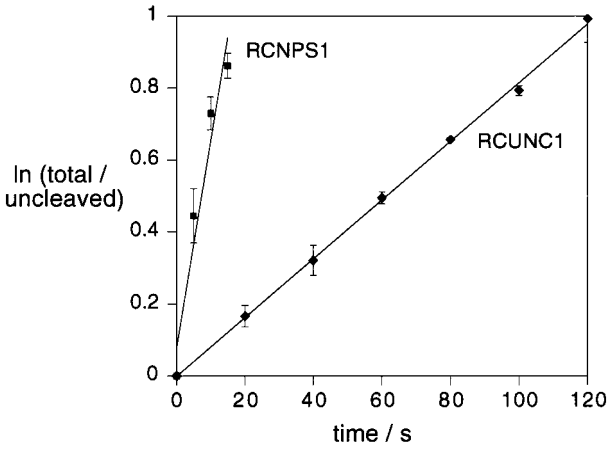

FIGURE 7: RuvC cleavage of junctions containing a pre-existing strand break. Junctions RCUNC1 and RCNPS1 differ in that the latter contains a covalent break in the backbone at the point of strand exchange on the b strand. The data are presented as a plot of r strand cleavage progress as a function of time: intact junction [RCUNC1 (◆)] and nicked junction [RCNPS1 (■)]. The error bars are standard deviations of triplicate measurements.

Table 1: Rates of Cleavage of Synthetic DNA Junctions by RuvC[a]

junction	b strand sequence	rate ($\times 10^{-5}$ s^{-1})	r strand sequence	rate ($\times 10^{-5}$ s^{-1})
RCUNC1	ATG : GTG	713	ATT : CAG	762
RCUNC2	ATG : GTG	1.46	GCC : TAG	0.797
RCUNC3	GCC : TAG	5.5	ATT : CAG	420
RCUNC4	ATT : CAG	6120	ATT : CAG	6310
RCUNC5	ATG : GTG	77.9	AAT : TCA	1190

[a] The sequences at the cleavage sites on the b and r strands are shown, with the point of strand exchange indicated by the colon. Rates were measured under single-turnover conditions, in triplicate.

Table 2: Rates of Cleavage by RuvC of Synthetic DNA Junctions Containing Oligoadenine Bulges at the Point of Strand Exchange[a]

junction	b strand sequence	r strand sequence	rate (r strand) ($\times 10^{-5}$ s^{-1})
RCUNC1	ATG : GTG	ATT : CAG	762
RCUNC1BA1	ATG : A : GTG	ATT : CAG	3670
RCUNC1BA2	ATG : AA : GTG	ATT : CAG	1110
RCUNC1BA3	ATG : AAA : GTG	ATT : CAG	1090
RCUNC1BA4	ATG : AAAA : GTG	ATT : CAG	1560
RCUNC3	GCC : TAG	ATT : CAG	420
RCUNC3BA1	GCC : A : TAG	ATT : CAG	280
RCUNC3BA2	GCC : AA : TAG	ATT : CAG	206
RCUNC3BA3	GCC : AAA : TAG	ATT : CAG	528
RCUNC3BA4	GCC : AAAA : TAG	ATT : CAG	958
RCUNC3BA5	GCC : AAAAA : TAG	ATT : CAG	1110

[a] The sequences at the cleavage sites on the b and r strands are shown, including the oligoadenine sequences. Rates were measured under single-turnover conditions, in triplicate.

presence of divalent metal ions (*32*). The presence of oligoadenine bulges had a much smaller effect on binding affinity, with the bulged junctions being bound with equal or slightly increased affinity.

These results indicate that the change in cleavage rate is not due to changes in binding affinity. The reduced affinity for the nicked junction suggests that the acceleration observed in a junction containing a pre-existing strand break may be a lower limit, and that considerably greater accelerations should be possible in the case of a breakage produced in situ by the action of the enzyme itself.

DISCUSSION

Using a supercoil-stabilized cruciform structure containing RuvC target sequences, we have shown that RuvC introduces apparently simultaneous cleavages into the four-way DNA junction, with no accumulation of a unilaterally cleaved intermediate species. However, we have also shown that the two cleavages can be uncoupled if a heterodimer consisting of active and inactive subunits is used. Shah et al. (*31*) demonstrated uncoupling of the two cleavages when one of the scissile phosphates was replaced with a 3′-*S*-phosphorothiolate. These results indicate that RuvC has a mechanism by which paired bilateral cleavage is effectively ensured.

In previous studies with CCE1 and T4 endonuclease VII, we have observed the generation of a small fraction of the nicked junction as an intermediate in the resolution reaction (*20*). Kinetic analysis of the CCE1 cleavage process indicated that the two cleavages were sequential, with a rate for the subsequent cleavage that was accelerated by a factor of 5−10. Analogy with the other junction-resolving enzymes suggests that a similar mechanism would hold for RuvC, but simulation of the kinetic data indicates that the low level of nicked intermediate would require an acceleration of ≥100-fold. In an alternative mechanism, both cleavages might be fast, but were preceded by a slower conformational change in the enzyme−DNA complex. However, this possibility agrees less well with the data from the effects of sequence and strand discontinuities in isolated junctions, and is less consistent with observations on other junction-resolving enzymes. We have observed that the presence of an opposed strand break can greatly accelerate the cleavage at a given site. Introduction of bulged bases can also have a similar effect, suggesting that an increase in flexibility of the junction is the cause of the acceleration. Even greater rate increases for the second cleavages are observed when the first cleavage is introduced by the action of RuvC itself; a site that would be poorly cleaved in isolation can be cleaved 500 times faster when it opposes a rapidly cleaved RuvC site. The crystal structure of RuvC shows that the active sites of the two protomers are separated by ∼30 Å (*33*), which is too far to accommodate the scissile bonds simultaneously. This indicates that simultaneous cleavages are not brought about by the concerted action at the two sites, and would probably require a change in the global structure of the junction between cleavages.

According to the sequential cleavage model, the relationship between the two cleavages introduced by RuvC is qualitatively similar to that described previously for the yeast enzyme CCE1 (*20*), but the magnitude of the acceleration effect is much greater. We proposed a branched kinetic scheme in which the enzyme may cleave initially at either site to generate a nicked intermediate species, followed by the opposing cleavage to create a linear product. We use an equivalent scheme in the analysis of the present RuvC data (Figure 8A). The enzyme cleaves initially at site C (ATT↓C) or site G (ATT↓G) to generate a nicked intermediate. The enzyme must actively maintain the structure of the junction at this stage. Failure to do this would release the negative supercoiling; the cruciform would be reabsorbed, and none would remain to serve as the substrate for the second cleavage reaction. Under these circumstances, the DNA would remain in the nicked circular form, as is seen with

the active−inactive heterodimer species. For the fully active enzyme, the nicked species is subsequently cleaved at the opposing site, to generate the linear DNA product. We have shown (*20*) that the branched kinetic scheme leads to the following integrated rate equations:

$$[S]_t/[S]_0 = e^{-(k_1+k_2)t} \quad (1)$$

$$[N]_t/[S]_0 = \frac{k_1}{k_1+k_2-k_3}[e^{-k_3t} - e^{-(k_1+k_2)t}] + \frac{k_2}{k_1+k_2-k_4}[e^{-k_4t} - e^{-(k_1+k_2)t}] \quad (2)$$

$$[L]_t/[S]_0 = 1 - e^{-(k_1+k_2)t} - \frac{k_1}{k_1+k_2-k_3}[e^{-k_3t} - e^{-(k_1+k_2)t}] - \frac{k_2}{k_1+k_2-k_4}[e^{-k_4t} - e^{-(k_1+k_2)t}] \quad (3)$$

where $[S]_t$, $[N]_t$, and $[L]_t$ are the concentrations of supercoiled, nicked, and linear species at time t, respectively, and $[S]_0$ is the concentration of the supercoiled substrate at time zero. The fractions of these species for the cleavage of pRC1 by RuvC were quantified by fluorography, and are presented graphically in Figure 8B. The sum of the rate constants for the first cleavage ($k_1 + k_2$) was calculated by fitting the disappearance of the supercoiled substrate DNA, using eq 1. This was then divided into the individual cleavage rates at the C and G sites assuming that these would be in proportion to the rates of cleavage of isolated DNA junctions of the same sequence, giving the following values: $k_1 = 0.009\ s^{-1}$ and $k_2 = 0.002\ s^{-1}$. In our earlier studies of CCE1 cleavage (*20*), a significant fraction of nicked circular intermediate was present in the first minute of the reaction, and application of these equations to the experimental data led to the conclusion that the rate constants k_3 and k_4 were 5−10-fold greater than k_2 and k_1, respectively. In the case of RuvC, we do not observe a measurable fraction of nicked circular DNA generated at early reaction times, indicating that the acceleration of the second cleavage must be greater than that observed with CCE1. The small proportion of nicked circular DNA present does not exhibit kinetics consistent with eq 2, and low-level random nicking of supercoiled DNA is probably more important than RuvC action in the generation of this species. We therefore used the generation of the linear product to determine the rates of the second cleavage, i.e., k_3 and k_4. We assumed a uniform acceleration factor for second-strand cleavage (f), i.e., $k_3 = fk_2$ and $k_4 = fk_1$, and fitted the data to eq 3 on this basis. This generated the fit shown in Figure 8B. The acceleration factor producing the best fit (f) to the experimental data was 146. This represents an acceleration of the second cleavages relative to the first by 2 orders of magnitude. The effect can be compared with the relative rates for first and second strand cleavage by a restriction enzyme. In the case of *Bam*HI, the two rates have been found to be closely similar (*34*), in marked contrast to the case for the junction-resolving enzymes.

We proposed a model to account for the behavior of CCE1, in which the initial cleavage releases strain introduced into the junction on binding to the resolving enzyme. This strain could hinder the cleavage reaction, but upon being released by the first cleavage, the subsequent cleavage can proceed more efficiently, giving the observed acceleration. Both CCE1 (*35*, *36*) and RuvC (*37*) are known to distort the structure of the four-way junction on binding. Using isolated junctions, we have shown that the introduction of strand breaks and bulges that are known to increase flexibility into the structure can lead to significant acceleration of cleavage rates. If the strand break is introduced in situ by the action of RuvC, then an intrinsically poor site can be cleaved at a rate that is 500-fold faster than the rate for the site in isolation.

Our results indicate that an intimate relationship exists between the structure of the four-way junction and its resolution, and this is probably generally true. Four-way

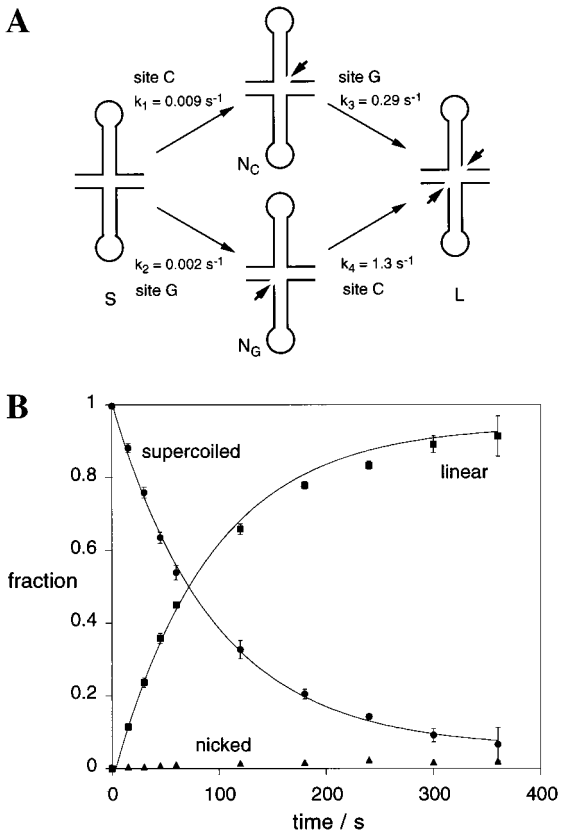

FIGURE 8: Kinetic analysis of RuvC cleavage. (A) The kinetic model used to analyze the data, and the calculated rate constants. This is based on a branched pathway. In the upper path, site C is cleaved initially with rate k_1 followed by site G (rate k_3). In the lower path, site G is cleaved first (rate k_2) followed by site C (rate k_4). The values of the rate constants were calculated by the fits to the experimental data. Note that k_4 and k_3 are 146-fold larger than k_1 and k_2, respectively, indicating that the rate of cleavage of a given site is accelerated once the first cleavage has been made. The indicated species are supercoiled DNA (S), linear DNA (L), and circular DNA nicked at the C (N_C) and G (N_G) sites. (B) Quantified data for RuvC cleavage of pRC1 and fitting of kinetic parameters based on the branched cleavage pathway. The points show the fractions of supercoiled (●), nicked (▲), and linear (■) pRC1 DNA measured experimentally at 47 °C. The error bars represent standard deviations of triplicate measurements. The lines shown are fits that were generated by nonlinear regression, using the integrated rate equations (eqs 1 and 3) given in the text. The very low level of nicked DNA prevented accurate fitting of these data; however, this is a further indication of the large rate enhancement for the second-strand cleavage reaction.

junctions are the central intermediate in the λ integrase family of site-specific recombination systems, and from crystallographic studies of the Cre recombinase with a four-way DNA junction based on the *loxP* site (*38*), van Duyne and colleagues have suggested that a change in the conformation of the junction determines the direction of resolution. In Xer recombination, the two sets of strand exchanges are catalyzed by different proteins, XerC and XerD (*39*), which are active at different stages of the overall process. Sherratt and coworkers (*40*) have proposed a mechanism by which interactions between the C-terminal regions cause changes in the conformation of the protein-bound junction that generate differential activation of the Xer proteins.

Effective coordination of first and second cleavage reactions is important for the biological function of the junction-resolving enzymes, because it makes productive resolution possible. If this did not occur, there would be a high probability that the junction would undergo branch migration between cleavages, leading to a junction with nicked arms and a failure of resolution. This problem may be especially acute for RuvC, as there is evidence that this may function as part of a "resolvasome" complex with the branch migration machinery RuvAB (*41*, *42*). Efficient branch migration in this form may require cleavages to be carried out in very quick succession to achieve a resolution of the junction, and the large acceleration for the second cleavage is likely to ensure this. Additionally, the kinetic properties of RuvC would also lead to resolution of any pre-existing nicks encountered by a moving junction.

MATERIALS AND METHODS

Preparation of Supercoiled Plasmid DNA. The principle of the construction of pRC1 is discussed in the Results. The DNA was transformed into *E. coli* DH5α, and the bacteria were grown to an A_{600} of 0.6. The plasmid was amplified by treatment with 50 μg/mL chloramphenicol overnight. Plasmid DNA was isolated using the Wizard Maxiprep purification kit (Promega) and purified by isopycnic CsCl−ethidium bromide ultracentrifugation (*43*). Supercoiled DNA was recovered by side puncture. Ethidium bromide was removed by extraction into *n*-butanol and the DNA subjected to extensive dialysis to remove CsCl. This resulted in DNA containing >95% negatively supercoiled DNA as determined by agarose gel electrophoresis. DNA concentrations were measured spectrophotometrically. pRC1 was characterized by means of restriction analysis using *Alw*NI, *Ase*I (New England Biolabs), and *Sty*I (Promega).

Expression and Purification of RuvC. A *ruvC* gene was amplified from *E. coli* DNA using the polymerase chain reaction as described previously (*28*). Site-directed mutants of RuvC were obtained using the QuikChange system (Strategene). In brief, two oligonucleotide primers, each complementary to opposite strands of the inserted sequence in the pET19bRuvC expression plasmid, were extended during temperature cycling using *Pfu* DNA polymerase, generating a mutated plasmid containing staggered nicks. This was treated with *Dpn*I endonuclease to digest the parental DNA and to select for the mutated DNA. This plasmid was transformed into DH5α for sequencing to confirm the presence of the mutation. Wild-type RuvC and RuvC D7A were overexpressed in BL21(DE3) pLysS. Cells were grown to an absorbance A_{600} of 0.5 and induced by addition of IPTG to a final concentration of 0.05 mM for 2.5 h. Cells were harvested by centrifugation and lysed by sonication. The lysate was diluted 4-fold with 20 mM Tris-HCl (pH 7), 1 mM EDTA, 1 mM DTT, 200 mM NaCl, and 10% glycerol (buffer A) and applied to a SP-Sepharose column and eluted with buffer A supplemented with 2 M NaCl (buffer B). RuvC-containing fractions were applied to a POROS HS 20/100 ion-exchange column and eluted with a 200 mM to 2 M NaCl gradient in 10 mM MES (pH 6), 1 mM EDTA, 1 mM DTT, and 10% glycerol. RuvC-containing fractions were concentrated and applied to a Superose-12 gel filtration column (Pharmacia) and eluted isocratically. RuvC in peak fractions was essentially pure as observed by SDS−PAGE, and no nonspecific nuclease activity could be detected.

Cleavage of Plasmid DNA by RuvC. Plasmid pRC1 DNA (20 nM) was incubated with a range of concentrations of RuvC in 20 mM Tris-HCl (pH 8.0), 20 mM NaCl, 0.1 mg/mL BSA, and 0.2 mM DTT (RuvC reaction buffer) at 37 °C. $MgCl_2$ was added to a final concentration of 15 mM in a total volume of 10 μL. The reactions were terminated after 5 min by addition of a solution containing 250 mM EDTA and 1 mg/mL proteinase K and incubated for >20 min to digest any RuvC still bound to the DNA before electrophoresis.

Time Course of the RuvC Cleavage Reaction. pRC1 DNA was incubated with 1 μM RuvC in RuvC reaction buffer at 47 °C. Reactions were initiated by addition of $MgCl_2$ to a final concentration of 15 mM in a volume of 50 μL. Aliquots (5 μL) were removed at intervals and added to a solution containing 250 mM EDTA and 1 mg/mL proteinase K, and the mixtures were incubated for >20 min before electrophoresis was carried out. The higher temperature was used in these experiments because incomplete cleavage had been observed at lower temperatures.

Cleavage Reactions with Heterodimeric RuvC. A range of mixtures of wild-type RuvC and catalytically inactive RuvC giving a constant final concentration of wild-type enzyme (250 nM) and an increasing mole fraction of mutant enzyme were incubated together for 60 min at 20 °C to allow subunit exchange. After addition of DNA in reaction buffer, $MgCl_2$ was added to a final concentration of 15 mM in a volume of 10 μL. Samples were incubated at 47 °C for 10 min. Reactions were terminated by addition of a solution containing 250 mM EDTA and 1 mg/mL proteinase K and the mixtures incubated for 20 min before electrophoresis.

Analysis of Cleavage Products. Samples were loaded onto a 1% agarose gel and electrophoresed for 16 h at 30 V in TBE buffer. DNA was stained using 5 μg/mL ethidium bromide. After destaining in water, gels were scanned using a FLA-2000 fluorescent image analyzer (Fuji) using excitation at 473 nm with an emission filter at 580 nm, and quantified using Mac-Bas software (Fuji).

Construction of Four-Way Junctions. DNA junctions were constructed from four oligonucleotides termed b, h, r, and x sequentially around the center. The b strand was 30 nucleotides and the r strand 40 nucleotides in length, and the h and x strands were 35 nucleotides in length. The b and r strands of each junction were radioactively labeled with [γ-^{32}P]ATP and T4 polynucleotide kinase. Stoichiometric quantities of these strands and the two unlabeled strands were

annealed by incubation in 50 mM Tris-HCl (pH 7.6), 10 mM $MgCl_2$, 5 mM DTT, 0.1 M spermine, and 0.1 mM EDTA for 3 min at 85 °C followed by slow cooling. Junctions were purified by electrophoresis in 5% polyacrylamide; bands were excised, and the DNA was recovered by electroelution followed by ethanol precipitation. Junctions were assembled with the following sequences together with other strands where indicated. All sequences are written 5′ to 3′.

Junction RCUNC1: b strand, TCCGTCCTAGCAATGGTGTGCTACCGGAAG; h strand, CTTCCGGTAGCACACAATCCGGTGGTTGAATTCCT; r strand, AGGAATTCAACCACCGGATTCAGGAACTGCAGTCTAGACT; and x strand, AGTCTAGACTGCAGTTCCTGCATTGCTAGGACGGA. Junction RCUNC2: b strand, from RCUNC1; h strand, CTTCCGGTAGCACACGGCCCGGTGGTTGAATTCCT; r strand, AGGAATTCAACCACCGGGCCTAGGAACTGCAGTCTAGACT; and x strand, AGTCTAGACTGCAGTTCCTACATTGCTAGGACGGA. Junction RCUNC3: b strand, TCCGTCCTAGCAGCCTAGTGCTACCGGAAG; h strand, CTTCCGGTAGCACTAAATCCGGTGGTTGAATTCCT; r strand, from RCUNC1; and x strand, AGTCTAGACTGCAGTTCCTGGGCTGCTAGGACGGA. Junction RCUNC4: b strand, TCCGTCCTAGCAATTCAGTGCTACCGGAAG; h strand, CTTCCGGTAGCACTGAATCCGGTGGTTGAATTCCT; r strand, AGGAATTCAACCACCGGATTCAGGAACTGCAGTCTAGACT; and x strand, AGTCTAGACTGCAGTTCCTGAATTGCTAGGACGGA. Junction RCUNC5: b strand, TCCGTCCTAGCAATGGTGTGCTACCGGAAG; h strand, CTTCCGGTAGCACACATTCCGGTGGTTGAATTCCT; r strand, AGGAATTCAACCACCGGAATTCAGAACTGCAGTCTAGACT; and x strand, AGTCTAGACTGCAGTTCTGACATTGCTAGGACGGA. Junction RCUNC1 (long version for junction containing strand breaks): b strand, CGCTTTCCGTCCTAGCAATGGTGTGCTACCGGAAGGATCT; h strand, AGATCCTTCCGGTAGCACACAATCCGGTGGTTGAATTCCTAGGGACCTAG; r strand, CTAGGTCCCTAGGAATTCAACCACCGGATTCAGGAACTGCAGTCTAGACTAAGGAGTCTG; and x strand, CAGACTCCTTAGTCTAGACTGCAGTTCCTGCATTGCTAGGACGGAAAGCG.

Construction of Four-Way Junctions Containing Strand Breaks and Extra Bases. Junctions containing strand breaks were constructed by replacing one of the strands with two oligonucleotides corresponding to the two parts of the nicked strand. The length of the arms of the four-way junction was increased to stabilize the nicked junction (40-nucleotide b strand, 60-nucleotide r strand, and 50-nucleotide h and x strands). Bulged junctions were constructed by the addition of up to five adenine nucleotides in the b strand at the position of strand exchange. Junctions were radioactively labeled, annealed, and purified as described previously.

Single-Turnover Kinetic Analysis of Junction Cleavage. Rates of DNA junction cleavage were measured under single-turnover conditions, using 80 nM radioactively labeled junction and 1 μM RuvC in RuvC reaction buffer in a total volume of 30 μL. Under these conditions, all junction should be bound to RuvC. Samples were pre-equilibrated at 37 °C and the cleavage reactions initiated by addition of $MgCl_2$ to a final concentration of 15 mM. At set time points, aliquots were removed and added to an equal volume of 95% (v/v) formamide, 50 mM EDTA (pH 8.0), 0.1% xylene cyanol, and 0.1% bromophenol blue and heated at 90 °C for 4 min followed by storage on ice. Reaction products were analyzed by denaturing gel electrophoresis in 12% polyacrylamide gels containing 7 M urea run at 50 °C in TBE buffer. Gels were exposed to storage phosphor screens, and the radioactivity was quantified using a Fuji-BAS 1500 phosphorimager and Mac-BAS software (Fuji). Since the b and r strands of the junction were of different lengths, the time courses of cleavage of the two different strands could be observed on the same gel. First-order rate constants were obtained by measuring the gradient of ln(total/uncut) against time by linear regression. All rate measurements were performed in triplicate, from which mean rate constants and standard deviations were calculated.

Measurement of the Binding Affinity of RuvC for DNA Junctions. A range of concentrations of RuvC was incubated with 0.25 nM radioactively labeled four-way DNA junctions for 15 min in 20 mM Tris-HCl (pH 8.0), 20 mM NaCl, 0.1 mg/mL BSA, 1 mM DTT, and 1 mM EDTA (RuvC binding buffer) in a total volume of 10 μL. One-sixth volume of 0.25% bromophenol blue, 0.1% xylene cyanol, and 35% Ficoll type 40 was added, and the samples were loaded onto 5% polyacrylamide gels. After electrophoresis in TBE buffer for approximately 2 h, the gels were dried and exposed to storage phosphor screens for phosphorimaging as described above. Data were analyzed as previously described (*28*).

ACKNOWLEDGMENT

We thank Anne-Cécile Déclais, Malcolm White, and Mamuka Kvaratskhelia for helpful discussions.

REFERENCES

1. Holliday, R. (1964) *Genet. Res. 5*, 282−304.
2. Broker, T. R., and Lehman, I. R. (1971) *J. Mol. Biol. 60*, 131−149.
3. Orr-Weaver, T. L., Szostak, J. W., and Rothstein, R. J. (1981) *Proc. Natl. Acad. Sci. U.S.A. 78*, 6354−6358.
4. Potter, H., and Dressler, D. (1976) *Proc. Natl. Acad. Sci. U.S.A. 73*, 3000−3004.
5. Schwacha, A., and Kleckner, N. (1995) *Cell 83*, 783−791.
6. White, M. F., Giraud-Panis, M.-J. E., Pöhler, J. R. G., and Lilley, D. M. J. (1997) *J. Mol. Biol. 269*, 647−664.
7. Kemper, B., and Garabett, M. (1981) *Eur. J. Biochem. 115*, 123−131.
8. de Massey, B., Studier, F. W., Dorgai, L., Appelbaum, F., and Weisberg, R. A. (1984) *Cold Spring Harbor Symp. Quant. Biol. 49*, 715−726.
9. Connolly, B., Parsons, C. A., Benson, F. E., Dunderdale, H. J., Sharples, G. J., Lloyd, R. G., and West, S. C. (1991) *Proc. Natl. Acad. Sci. U.S.A. 88*, 6063−6067.
10. Iwasaki, H., Takahagi, M., Shiba, T., Nakata, A., and Shinagawa, H. (1991) *EMBO J. 10*, 4381−4389.
11. West, S. C., Parsons, C. A., and Picksley, S. M. (1987) *J. Biol. Chem. 262*, 12752−12758.
12. Symington, L., and Kolodner, R. (1985) *Proc. Natl. Acad. Sci. U.S.A. 82*, 7247−7251.
13. White, M. F., and Lilley, D. M. J. (1997) *Mol. Cell. Biol. 17*, 6465−6471.
14. Elborough, K. M., and West, S. C. (1990) *EMBO J. 9*, 2931−2936.
15. Stuart, D., Ellison, K., Graham, K., and McFadden, G. (1992) *J. Virol. 66*, 1551−1563.
16. Komori, K., Sakae, S., Shinagawa, H., Morikawa, K., and Ishino, Y. (1999) *Proc. Natl. Acad. Sci. U.S.A. 96*, 8873−8878.
17. Kvaratskhelia, M., and White, M. F. (2000) *J. Mol. Biol. 295*, 193−202.

18. Giraud-Panis, M.-J. E., and Lilley, D. M. J. (1997) *EMBO J. 16*, 2528−2534.
19. Parkinson, M. J., and Lilley, D. M. J. (1997) *J. Mol. Biol. 270*, 169−178.
20. Fogg, J. M., Schofield, M. J., Déclais, A.-C., and Lilley, D. M. J. (2000) *Biochemistry 39*, 4082−4089.
21. Gellert, M., Mizuuchi, K., O'Dea, M. H., Ohmori, H., and Tomizawa, J. (1979) *Cold Spring Harbor Symp. Quant. Biol. 43*, 35−40.
22. Lilley, D. M. J. (1980) *Proc. Natl. Acad. Sci. U.S.A. 77*, 6468−6472.
23. Panayotatos, N., and Wells, R. D. (1981) *Nature 289*, 466−470.
24. Mizuuchi, K., Kemper, B., Hays, J., and Weisberg, R. A. (1982) *Cell 29*, 357−365.
25. Lilley, D. M. J., and Kemper, B. (1984) *Cell 36*, 413−422.
26. Mizuuchi, K., Mizuuchi, M., and Gellert, M. (1982) *J. Mol. Biol. 156*, 229−243.
27. Lilley, D. M. J., and Hallam, L. R. (1984) *J. Mol. Biol. 180*, 179−200.
28. Fogg, J. M., Schofield, M. J., White, M. F., and Lilley, D. M. J. (1999) *Biochemistry 38*, 11349−11358.
29. Shah, R., Bennett, R. J., and West, S. C. (1994) *Cell 79*, 853−864.
30. Greaves, D. R., Patient, R. K., and Lilley, D. M. J. (1985) *J. Mol. Biol. 185*, 461−478.
31. Shah, R., Cosstick, R., and West, S. C. (1997) *EMBO J. 16*, 1464−1472.
32. Pöhler, J. R. G., Duckett, D. R., and Lilley, D. M. J. (1994) *J. Mol. Biol. 238*, 62−74.
33. Ariyoshi, M., Vassylyev, D. G., Iwasaki, H., Nakamura, H., Shinagawa, H., and Morikawa, K. (1994) *Cell 78*, 1063−1072.
34. Hensley, P., Nardone, G., Chirikjian, J. G., and Wastney, M. E. (1990) *J. Biol. Chem. 265*, 15300−15307.
35. White, M. F., and Lilley, D. M. J. (1997) *J. Mol. Biol. 266*, 122−134.
36. Déclais, A.-C., and Lilley, D. M. J. (2000) *J. Mol. Biol. 296*, 421−433.
37. Bennett, R. J., and West, S. C. (1995) *J. Mol. Biol. 252*, 213−226.
38. Guo, F., Gopaul, D. N., and Van Duyne, G. D. (1999) *Proc. Natl. Acad. Sci. U.S.A. 96*, 7143−7148.
39. Blakely, G. W., and Sherratt, D. J. (1994) *Nucleic Acids Res. 22*, 5613−5620.
40. Hallet, B., Arciszewska, L. K., and Sherratt, D. J. (1999) *Mol. Cell 4*, 1−20.
41. Zerbib, D., Mézard, C., George, H., and West, S. C. (1998) *J. Mol. Biol. 281*, 621−630.
42. van-Gool, A. J., Hajibagheri, N. M., Stasiak, A., and West, S. C. (1999) *Genes Dev. 13*, 1861−1870.
43. Murchie, A. I. H., and Lilley, D. M. J. (1992) *Methods Enzymol. 211*, 158−180.

BI001886M